

The sweeping rate in diffusion-mediated reactions on dust grain surfaces

I. Lohmar and J. Krug

Institut für theoretische Physik, Universität zu Köln, Zùlpicher Str. 77, 50937 Köln, Germany

29 September 2018

ABSTRACT

A prominent chemical reaction in interstellar clouds is the formation of molecular hydrogen by recombination, which essentially takes place on dust grain surfaces. Analytical approaches to model such a system have hitherto neglected the spatial aspects of the problem by employing a simplistic version of the sweeping rate of reactants. We show how these aspects can be accounted for by a consistent definition of the sweeping rate, and calculate it exactly for a spherical grain. Two regimes can be identified: Small grains, on which two reactants almost surely meet, and large grains, where this is very unlikely. We compare the true sweeping rate to the conventional approximation and find a characteristic reduction in both regimes, most pronounced for large grains. These effects can be understood heuristically using known results from the analysis of two-dimensional random walks. We finally examine the influence of using the true sweeping rate in the calculation of the efficiency of hydrogen recombination: For fixed temperature, the efficiency can be reduced considerably, and relative to that, small grains gain in importance, but the temperature window in which recombination is efficient is not changed substantially.

Key words: astrochemistry – molecular processes – methods: analytical – diffusion – ISM: clouds – ISM: molecules

1 INTRODUCTION

The complex chemistry of interstellar clouds originates from reactions taking place both in the gas phase and on the surfaces of dust grains. The most important surface reaction is the formation of molecular hydrogen, which is highly inefficient in the gas phase (Vidali et al. 2005). Accordingly, there has been much recent interest in developing accurate and efficient methods for the modelling of chemical reactions taking place on dust grain surfaces (Herbst & Shematovich 2003). The most widespread approach for treating networks involving both surface and gas phase reactions is based on chemical rate equations, where the populations of different species are described by continuous concentration variables and the rate of production of a species is proportional to the product of the concentrations of its constituents (Pickles & Williams 1977).

However, rate equations become inappropriate for small grains subject to low fluxes of reactants, because the concept of a continuous concentration is questionable when the typical number of reactants on a grain drops below unity (Charnley et al. 1997; Caselli et al. 1998). In this regime it is necessary to consider the full probability distribution $P(N)$ of the number of reactants N on the grain (say, the number of H atoms), either within a stochastic Monte

Carlo simulation (Tielens & Hagen 1982; Stantcheva et al. 2001) or by solving the master equation governing the time evolution of $P(N)$ (Green et al. 2001; Biham et al. 2001; Biham & Lipshtat 2002; Lipshtat & Biham 2004).

None of the three modelling approaches mentioned above takes explicit account of the process by which reactants migrate and meet on the grain surface, through thermal hopping or quantum tunnelling. All such spatial aspects of the problem are instead lumped into the *sweeping rate* A , which is usually defined as the inverse of the time required for a single atom to visit all S adsorption sites on the grain, and is taken to be of the form (Stantcheva et al. 2001)

$$A = a/S \tag{1}$$

where a denotes the rate of hops between neighboring adsorption sites. This expression is problematic for two reasons. First, since a random walker in two dimensions occasionally revisits a site, it requires more than S hops to explore the entire surface (Montroll & Weiss 1965; Hughes 1995; Krug 2003). Second, and more fundamentally, the actual process of interest – the joint diffusion of two atoms which terminates when either one of them desorbs, or the two meet and react – is distinct from, and not simply related to, the exploration of the grain by a single atom. To the best of our knowledge, so far the only approach that overcomes

arXiv:astro-ph/0604021v1 3 Apr 2006

these limitations is the fully microscopic Monte Carlo simulation of the hopping and reaction of molecules on the lattice of adsorption sites (Chang et al. 2005; Cuppen & Herbst 2005), which cannot be used for the modelling of large reaction networks over long times.

The goal of this paper is to provide a consistent definition of the true sweeping rate, and to show how it can be evaluated exactly for a spherical grain. In Sect. 2 we establish a transparent interpretation of the sweeping rate and express it in terms of the encounter probability of a pair of atoms on the grain. This encounter probability is calculated for a spherical grain in Sect. 3, and two regimes of parameters are identified, for which there are simple approximate results. This section also highlights a quantitative relation between the encounter probability and the deviation of the distribution of the number of reactants on the grain from a Poisson distribution. In Sect. 4 the results are used to obtain the true sweeping rate in terms of physical parameters, which is then compared to the conventional approximation. We find that the true sweeping rate is reduced considerably, and the effect is most pronounced for large grains. Random walk considerations are employed to reproduce asymptotically exact expressions. We then examine the effect of using the true sweeping rate on the recombination efficiency (as a function of grain size and of grain temperature) in Sect. 5, for a set of physical parameters that has been used in other work, and that enables us to compare our results to those of microscopic Monte Carlo simulations. A summary and our conclusions are presented in Sect. 6.

We focus the discussion on the specific case of hydrogen recombination, but expect the results to be relevant also for other, more complex diffusion-mediated reactions.

2 BASIC RELATIONS AND DEFINITIONS

We consider a grain subject to a flux F of H atoms per unit time, which can desorb at rate W . Once formed, molecular hydrogen is assumed to desorb rapidly, or at least not to affect the diffusion and reaction of H atoms. The standard rate equation governing the mean number $\langle N \rangle$ of H atoms on the grain then reads (Biham et al. 1998)

$$\frac{d\langle N \rangle}{dt} = F - W\langle N \rangle - 2A\langle N \rangle^2. \quad (2)$$

The sweeping rate A appears in the last term on the right hand side, which contains the key approximation inherent in the rate equation method, i.e. setting the reaction rate proportional to the product of the mean numbers of reactants. Since each reaction consumes two atoms, the recombination rate is thus taken to be

$$R_{\text{rateeq}} = A\langle N \rangle^2. \quad (3)$$

Within the master equation treatment, this is replaced by the expression (Green et al. 2001; Biham et al. 2001; Biham & Lipshtat 2002)

$$R_{\text{master}} = A\langle N(N-1) \rangle, \quad (4)$$

which correctly accounts for the fact that the reaction rate is proportional to the number of *pairs* of atoms, and hence vanishes when $N = 1$. Equations (3) and (4) are seen to be identical whenever $\langle N^2 \rangle - \langle N \rangle^2 = \langle N \rangle$, i.e. when the

variance of the distribution $P(N)$ of the reactant number equals its mean. This is a defining property of the Poisson distribution, which holds irrespective of the mean of the distribution.

The comparison of (3) and (4) shows that a failure of the rate equation approach, in the sense of a large discrepancy between the two expressions, is not necessarily implied when the mean number of H atoms $\langle N \rangle$ becomes small compared to unity (Biham et al. 2005). The rate equation can be safely applied to any arbitrarily small region of a macroscopic surface, as long as atoms can freely enter and exit to ensure that the Poisson statistics of the number of reactants in the region is maintained. Rather, the failure of the rate equation (2) on small grains is a consequence of the *confinement* of the reactants on the grain surface, which implies that every adsorption site is visited many times and the probability for the two reactants to meet is sharply enhanced. As a consequence, the probability to find two atoms simultaneously on the grain is strongly reduced compared to the Poisson distribution, and $R_{\text{master}} \ll R_{\text{rateeq}}$. A precise quantitative relation between the encounter probability for two atoms and the deviation of $P(N)$ from a Poisson distribution will be given below in Sect. 3.4.

The expression (4) provides a transparent interpretation of the sweeping rate A : Since the number of pairs of atoms on the grain is $N(N-1)/2$, $2A$ is the rate at which *pairs of atoms are removed by the reaction*. The alternative pathway for a pair to disappear is through the desorption of one of its constituents, which occurs at rate $2W$. We conclude that the probability p_{enc} for a pair of atoms to meet and react before one of them desorbs is given by

$$p_{\text{enc}} = \frac{2A}{2A + 2W} = \frac{A}{A + W}. \quad (5)$$

Conversely, the relation (5) can be used to express the sweeping rate in terms of p_{enc} as

$$A = \frac{Wp_{\text{enc}}}{1 - p_{\text{enc}}}. \quad (6)$$

In the next section we show how p_{enc} can be computed analytically in terms of the model parameters.

3 ENCOUNTER PROBABILITY

Since the confined geometry plays an important role for the sweeping rate, we need to specify the shape of the grain. We will treat the simplest case of a sphere, which has the crucial advantage that all adsorption sites are equivalent. This is in contrast e.g. to the disc geometry employed previously in a similar calculation (Krug 2003).

The definition of the encounter probability involves a pair of atoms, each of which hops to adjacent adsorption sites at rate a and desorbs at rate W . Because of translational invariance on the surface of the sphere, this situation is equivalent to that of a single particle moving with the double hopping rate $2a$ and desorbing at twice the rate $2W$, while the other atom remains fixed and present all the time. As we are only concerned with the encounter probability (as opposed to the time of encounter), multiplying both rates by a common factor of 2 does not change the result [compare to (5)]; hence we revert to the original rates a and W for

the moving particle and keep the second particle fixed and present throughout.

3.1 Stationary diffusion problem

Following the approach of Krug (2003), the next step consists in passing to a continuum limit in which the occupation probability $n(\mathbf{x})$ of the moving atom satisfies a stationary diffusion equation. The spherical grain has a radius R , while the fixed ‘target atom’ is modelled as a circular surface area of radius r , located at the north pole of the sphere. Since we assume the grain to be large enough to contain at least a few hundred adsorption sites, $r \ll R$. In the original discrete setting the sphere is tiled by adsorption sites forming some regular lattice. The radius r of the target atom then corresponds to a distance of $2r$ between adjacent adsorption sites. In the appendix A it is shown for some common lattice structures that the number of adsorption sites is given by

$$S = g(2R/r)^2, \quad (7)$$

where the factor $g = \mathcal{O}(1)$ reflects the lattice geometry.

The diffusion constant D for a two-dimensional random walk on the lattice of adsorption sites is related to the hopping rate a by $D = a(\delta x)^2/4$, where $\delta x = 2r$ is the length of a single step, and hence $D = ar^2$ (Michely & Krug 2004). We thus arrive at the stationary diffusion equation

$$D\nabla^2 n + \frac{F}{4\pi R^2} - Wn = 0 \quad (8)$$

describing the occupation probability n of the moving atom in the steady state of impingement, desorption and reaction. To utilise the azimuthal symmetry of the problem we go to spherical polar coordinates, writing the Laplace operator in the form

$$\nabla^2 = \frac{1}{R^2 \sin \theta} \frac{\partial}{\partial \theta} \sin \theta \frac{\partial}{\partial \theta}. \quad (9)$$

The reaction removing the pair of atoms is accounted for by an absorbing boundary condition at the boundary of the fixed atom,

$$n(\theta = r/R) = 0. \quad (10)$$

3.2 Exact solution

The non-negative solution of (8, 10) that is finite at the south pole $\theta = \pi$ is found after transforming to the new variable $z = \cos \theta$, and is given in terms of Legendre functions of the first kind $P_\nu(z)$ by¹

$$n(\theta) = \frac{F}{4\pi R^2 W} \left[1 - \frac{P_\nu(-\cos \theta)}{P_\nu(-\cos(r/R))} \right], \quad (11)$$

where the index reads

$$\nu = -\frac{1}{2} + \sqrt{\frac{1}{4} - \left(\frac{R}{\ell_D}\right)^2}, \quad (12)$$

¹ Mathematical details can be found in Gradshteyn & Ryzhik (2000), sections 8.7 and 8.8, especially 8.706f., 8.823 and 8.840 to 8.842. Note that, although the index ν can become complex, all physical expressions are real.

and we have introduced the *diffusion length*

$$\ell_D = \sqrt{D/W}. \quad (13)$$

This is the typical distance an atom on an unbounded surface would diffuse prior to desorbing.

The encounter probability for the pair of atoms (already averaged over all possible starting points) then consists of two parts. The first part is given by the fraction of all impinging atoms that reach the target by diffusion, that is the fraction of the impingement flux F that enters the target as a diffusion flux:

$$p_{\text{diff}} = 2\pi R \sin(r/R) \times \frac{D}{R} \frac{\partial n}{\partial \theta} \Big|_{\theta=r/R} \times \frac{1}{F}. \quad (14)$$

Using a well-known identity² this yields

$$p_{\text{diff}} = \frac{\sin(r/R)}{2(R/\ell_D)^2} \frac{P'_\nu(-\cos(r/R))}{P_\nu(-\cos(r/R))}, \quad (15)$$

where $P'_\nu = -(1-z^2)^{1/2} dP_\nu/dz$. However, a (small) fraction of atoms impinges directly on top of the target area, and these are responsible for an additional contribution to the encounter probability, namely the (purely geometrical) ratio $u \equiv (1 - \cos(r/R))/2$ of the target versus the total surface area.³

The overall encounter probability of a pair of atoms therefore is

$$p_{\text{enc}} = \frac{\sin(r/R)}{2(R/\ell_D)^2} \frac{P'_\nu(-\cos(r/R))}{P_\nu(-\cos(r/R))} + \frac{1 - \cos(r/R)}{2}. \quad (16)$$

Equation (16) is the central result of this section. It should be emphasised that the encounter probability is independent of the impingement flux because it only contains information about two atoms that are already assumed to be present on the grain. The following section will feature the behaviour of the encounter probability in the regimes of physical interest.

3.3 Limiting behaviour

We will first derive the approximate behaviour common to all relevant regimes (as defined by the ordering of the three length scales, r , R and ℓ_D). It was mentioned earlier that $r \ll R$ is necessary for the dust grain to host a reasonable number of adsorption sites. But clearly, $r \ll \ell_D$ as well, because otherwise the adatom hardly performs any hops during its residence time on the grain. In terms of the parameters of (16) the common feature of all regimes is that $r/R \ll 1$, thus being the appropriate quantity in which to expand first.

The actual calculation involves some subtleties, and we relegate most of this to appendix B. To leading order in r/R ,

² Gradshteyn & Ryzhik (2000), equation 8.752, 1.

³ Although this term is of the order of $(r/R)^2 \ll 1$, we found it must be accounted for in certain situations. The essential reason for this is that, while $u \ll p_{\text{diff}} < p_{\text{enc}}$ is valid in *all* regimes of interest, we will also be concerned with the complementary quantity $1 - p_{\text{enc}}$ appearing in (6). This however can become arbitrarily small, and particularly of the order of u or smaller. Appendix B will show that inclusion of u even *simplifies* further analysis.

one obtains⁴

$$p_{\text{enc}}^{-1} \approx \left(\frac{R}{\ell_{\text{D}}}\right)^2 \left[\ln\left(\frac{2R}{r}\right)^2 - 2\gamma - 2\psi(\nu+1) - \pi \cot(\nu\pi) \right]. \quad (17)$$

Here $\psi(z) \equiv d(\ln\Gamma)/dz$, where $\Gamma(z)$ is the Γ -function, and $\gamma = -\psi(1) \approx 0.577215665\dots$ is Euler's constant. To gain insight into the behaviour of the encounter probability it is useful to examine the two remaining regimes in which r is the smallest length scale of the problem. The relation between the grain radius R and the diffusion length ℓ_{D} conveys a notion of 'small' and 'large' grains.

3.3.1 Small grains

Here, the ordering of lengths reads $r \ll R \ll \ell_{\text{D}}$ and hence $|\nu| \ll 1$. Expanding p_{enc} about $\nu \rightarrow 0^-$ to first order yields $p_{\text{enc}} \approx 1 + \nu[\ln(2R/r)^2 - 1]$, and with $\nu \approx -(R/\ell_{\text{D}})^2$ we have⁵

$$p_{\text{enc}} \approx 1 - \left(\frac{R}{\ell_{\text{D}}}\right)^2 \left[\ln\left(\frac{2R}{r}\right)^2 - 1 \right] \rightarrow 1. \quad (18)$$

In this regime of low desorption rate each atom spends enough time on the grain to explore all adsorption sites many times. For low fluxes, the recombination efficiency is then limited by the rare event that two atoms are simultaneously present on the grain. In this event however, they almost surely meet. It is for encounter probabilities near unity that the failure of the rate equation description is most pronounced, see Sect. 3.4.

3.3.2 Large grains

Now, $r \ll \ell_{\text{D}} \ll R$ and $\nu = -1/2 + i\lambda$ with $\lambda \approx R/\ell_{\text{D}} \gg 1$. For this form of ν , the cotangent in (17) is purely imaginary and cancels the imaginary part of $\psi(\nu+1)$ (cf. footnote 4). The behaviour of the Γ -function implies $\psi(z) \approx \ln z + \mathcal{O}(z^{-1})$ for arguments of large modulus, leading to $\text{Re}\psi(\nu+1) \approx \ln(R/\ell_{\text{D}})$ for the remaining real part of ψ . Together we obtain

$$p_{\text{enc}} \approx \left(\frac{\ell_{\text{D}}}{R}\right)^2 \frac{1}{\ln(2\ell_{\text{D}}/r)^2 - 2\gamma} \ll 1. \quad (19)$$

For low fluxes this means that the recombination efficiency is low because of fast desorption, which does not allow the atoms to spend sufficient time on the grain to react. This is the *second order* regime of Biham & Lipshtat (2002) and Krug (2003), in which the confinement of the atoms to the grain surface is not felt, and hence the rate equation continues to apply even for small numbers of reactants. In both limits, (18) and (19), the functional dependence on the model parameters is the same as that found earlier for the

disc geometry (Krug 2003), taking into account that there, logarithms of large arguments are generally assumed large as well (dominating possible numerical constants of the order of unity).

3.4 Non-Poissonian statistics

In this section we derive a simple quantitative relation between the encounter probability and the deviation of $P(N)$ from a Poisson distribution, in the limit where the mean number of reactants on the grain is small ($\langle N \rangle \ll 1$). In this regime the distribution $P(N)$ can be truncated at $N = 2$. Hence $\langle N \rangle \approx P(1) + 2P(2)$ and $\langle N^2 \rangle \approx P(1) + 4P(2)$, which implies that the recombination rate (4) is given by

$$R_{\text{master}} \approx 2AP(2). \quad (20)$$

Alternatively, R_{master} can be evaluated for $\langle N \rangle \ll 1$ using the following simple statistical argument (Krug et al. 2000; Krug 2003): An atom arriving freshly on the grain will participate in a reaction if, first, another atom is already present [which is true with probability $P(1)$] and, second, if the two encounter each other (which is true with probability p_{enc}). Multiplying this with the total flux of atoms onto the grain, we have

$$R_{\text{master}} \approx FP(1)p_{\text{enc}} \approx WP(1)^2p_{\text{enc}}. \quad (21)$$

In the second step we have used that, to leading order for $\langle N \rangle \rightarrow 0$, the mean number of atoms on the grain is $\langle N \rangle \approx F/W \approx P(1)$. Combining (20), (21) and (6) we arrive at the central relation

$$P(2) \approx \frac{1}{2}(1 - p_{\text{enc}})P(1)^2. \quad (22)$$

Since for the Poisson distribution $P(2) = P(1)^2/2$ for $\langle N \rangle \rightarrow 0$, we see that the factor $1 - p_{\text{enc}}$ is a quantitative measure for the deviation of $P(N)$ from the Poisson distribution, which reflects the depletion of the probability of pairs caused by the recombination reaction.

The relation (22) translates into a very simple expression for the deviation of the rate equation recombination rate (3) from the true rate (4). Indeed, for $\langle N \rangle \rightarrow 0$ the ratio of the two becomes

$$\frac{R_{\text{master}}}{R_{\text{rateeq}}} \approx 2P(2)/P(1)^2 \approx 1 - p_{\text{enc}}, \quad (23)$$

which highlights once more the importance of the confined grain geometry in the breakdown of the rate equation description. Using (24), the ratio (23) can be directly evaluated in terms of the physical parameters of the system.

4 SWEEPING RATE

We now translate our results back into the original language of the discrete picture via the relations $(2R/r)^2 = S/g$, $\ell_{\text{D}}/r = \sqrt{(D/r^2)/W} = \sqrt{a/W}$, and accordingly $R/\ell_{\text{D}} = \sqrt{SW/(4ga)}$. Rewriting the exact expression (16) for the encounter probability in these quantities is trivial, but only useful for the plots to come.

⁴ This approximation does not invalidate the reality of p_{enc} for values of ν of the form (12).

⁵ We will basically treat logarithms of large quantities as being of the order of unity throughout, thence retaining coequal numerical constants in sums, although the logarithms are usually significantly larger. While this might slightly blur the fundamental functional relation, it is numerically adequate in many realistic situations.

4.1 Sweeping rate for small and large grains

The regime of small grains is now characterized by $SW/a \ll 1$, with an encounter probability

$$p_{\text{enc}} \approx 1 - \frac{SW}{4ga} [\ln(S/g) - 1], \quad (24)$$

and the sweeping rate (6) becomes

$$A \approx \frac{W}{1 - p_{\text{enc}}} \approx \frac{4ga/S}{\ln(S/g) - 1}. \quad (25)$$

For large grains, given by $W/a \ll 1 \ll SW/a$, we have

$$p_{\text{enc}} \approx \frac{4ga}{SW} \frac{1}{\ln(4a/W) - 2\gamma}, \quad (26)$$

leading to a sweeping rate of

$$A \approx W p_{\text{enc}} \approx \frac{4ga/S}{\ln(4a/W) - 2\gamma}. \quad (27)$$

Compared to the conventional approximation (1), the sweeping rate is seen to be reduced by a logarithmic factor in both limits (the subtracted numerical constants in the preceding expressions will be ignored for the remaining discussion, cf. footnote 5).

In both cases, the argument of the logarithm is of the order of the number of all sites that the *second* (moving) atom has visited during its residence time. This behaviour is to be expected from random walk considerations for this moving atom (we still employ the scenario of the first H atom fixed and present throughout, as introduced at the beginning of Sect. 3): It is a known result for two-dimensional random walks that the mean number of *distinct* sites the atom has visited after time t (and thus, after at hops on average) is (asymptotically) given by

$$N_{\text{dis}} \approx \frac{\pi at}{C \ln(Bat)}, \quad (28)$$

with constants C and B depending on the type of lattice (Montroll & Weiss 1965; Hughes 1995). Note that this statement remains true if B is changed to *any* positive value, and accordingly, we will focus on the pre-factor depending on C . This constant has a value of $C = 1$ for a square, $C = \sqrt{3}/2$ for a triangular, and $C = 3\sqrt{3}/4$ for the hexagonal lattice, so that for our purposes, we can identify (cf. appendix A)

$$C = \pi/(4g). \quad (29)$$

The second ingredient of our reasoning is the effective residence time t_{res} of the moving atom in the two limits. If the encounter probability is very small (large grains), the atom explores only a small portion of the grain, and the residence time is (to first order in $a/(SW)$) limited by desorption, $t_{\text{res}} \approx 1/W$. The atom has therefore performed a/W hops and has visited $N_{\text{dis}} \approx 4g(a/W)/\ln(Ba/W)$ distinct sites. The encounter probability (which includes an average over all spatial initial conditions) is then given by the ratio N_{dis}/S , reproducing (26). This is the probability for the atom to recombine before it desorbs, which in this setting can as well be obtained as the recombination rate A times the residence time $1/W$, thereby yielding (27) once again.

If, on the other hand, the encounter probability is near unity (small grains), the stay of the atom is almost always ended by recombination, and the residence time becomes $t_{\text{res}} \approx 1/A$. By the same time, the atom has explored the

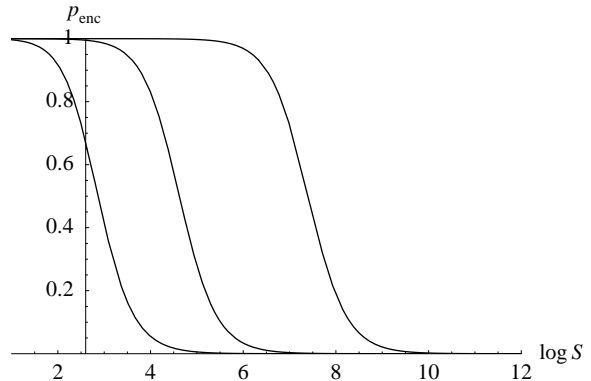


Figure 1. The encounter probability p_{enc} as a function of the grain size S (on a logarithmic scale to the basis of 10). The three graphs correspond (left to right) to $W/a = 10^{-3}$, 10^{-5} and 10^{-8} , and the grain size discriminating between small and large grains is then given by the inverse a/W . Starting at unity and monotonically decreasing, one can see the gentle roll-off of the encounter probability to take place around this critical size, yet of very similar shape in all three cases.

entire grain, so that the number of distinct sites visited has saturated at $N_{\text{dis}}(t_{\text{res}}) \approx S$. Inverting this relation one obtains (again to first order) $t_{\text{res}} \approx S \ln[SB/(4g)]/(4ga)$, thus reproducing the true sweeping rate (25). It is also easy to regain (24) without using the general relation (5): The probability for the atom to desorb before a reaction occurs can be written as $1 - p_{\text{enc}}$, but in this limit it is also given by the desorption rate W times the residence time $1/A$.

4.2 Comparison with the conventional approximation

We now want to illustrate the impact of the reduction factor that using the true sweeping rate implies. We will use the (appropriately translated) exact expression (16) for all plots throughout.

Evaluating the reduction factor of the true sweeping rate A compared to the conventional choice a/S by (6), we get

$$\frac{A}{a/S} = \frac{SW}{a} \frac{p_{\text{enc}}}{1 - p_{\text{enc}}}. \quad (30)$$

For the rest of this subsection we will not be concerned with the influence of the lattice structure, and hence will set $g = 1$. With the translation rules put forth at the beginning of Sect. 4, one can convince oneself that the only effect that a different lattice factor g has on the encounter probability is a rescaling of the grain size $S \rightarrow S/g$. It follows that, treating the reduction factor (30) as a function of the grain size, it is subject only to a rescaling of the variable and the value of the function (or a shift on a logarithmic scale, respectively).

Fig. 1 shows the encounter probability as a function of the grain size (on a logarithmic scale to the basis of 10) for three representative values of W/a . The ordinate crosses the abscissa at $S \approx 400$ (corresponding to $R/r \approx 10$) so that the region to the right of it is reasonably described by our model, cf. Sect. 3.1.

Fig. 2 presents (with the same conventions and for the same values of W/a) plots of the reduction factor $A/(a/S)$

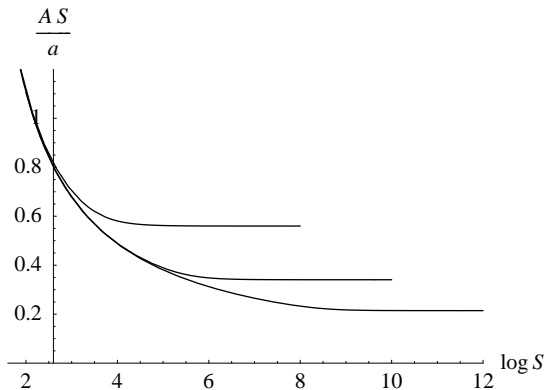


Figure 2. The reduction factor of the true sweeping rate versus the conventional approximation, with the same conventions as in Fig. 1 and for the same values (top to bottom) of W/a .

as a function of the grain size S . The graphs converge for (absolutely) small grains, because upon entering the small grain regime, the different parameter W/a does no longer affect $A/(a/S)$, cf. (25). With increasing grain size however, this reduction decreases to an asymptotic value depending on W/a . The approximations given in Sect. 4.1 for A as well as for p_{enc} are corroborated by these two figures.

It might come as a bit of a surprise that the reduction of the sweeping rate, while of serious account throughout, is most pronounced for *large*, not for small grains. This can, however, easily be understood: The key effect for the reduction of A as compared to a/S is back-diffusion, the revisiting of sites by a randomly walking atom. Small grains are those which are swept nearly entirely in most cases. This means that back-diffusion is rather ineffective in reducing the sweeping rate and corresponds to the observation that different values of W/a do not change the reduction factor in this regime – after all, recombination (not desorption) limits the residence time, anyway. The larger the grain surface becomes, the more does desorption compete with recombination as the limiting process. Therefore, there are more and more initial conditions for which back-diffusion is effective in reducing the sweeping rate. In the limit of large grains, desorption always ends the residence time. As a consequence, increasing S no longer increases the total number of sites an atom visits, and hence the effect of back-diffusion saturates as well, rendering $A/(a/S)$ constant (as a function of S).

In Sect. 3.4 it was shown that the reduction factor of the master equation versus the rate equation recombination rate (whenever $\langle N \rangle \ll 1$) exhibits the opposite behaviour (it is *only* relevant for small grains), because this reduction is based on a different aspect: The crucial point there was the ‘non-Poissonianity’ of $P(N)$ due to a large encounter probability, and ultimately owed to the confinement of the reactants to a small surface.

5 RECOMBINATION EFFICIENCY

A quantity that is more directly connected to observations of diffuse interstellar clouds is the recombination efficiency in the production of molecular hydrogen. It should therefore prove interesting to examine the effect that the use of the

reduced, true sweeping rate has on these quantities and to compare the results to recent simulations of the process. As the underlying analytic model we choose the master equation framework that is now generally agreed upon. It is given by

$$\begin{aligned} \frac{dP(N)}{dt} = & F [P(N-1) - P(N)] \\ & + W [(N+1)P(N+1) - NP(N)] \\ & + A [(N+2)(N+1)P(N+2) - N(N-1)P(N)] \end{aligned} \quad (31)$$

(with minor modifications for $N = 0, 1$). Green et al. (2001) and Biham & Lipshtat (2002) have independently found the analytic stationary solution, yielding

$$\langle N \rangle = \sqrt{\frac{F}{2A}} \frac{I_{W/A}(2\sqrt{2F/A})}{I_{W/A-1}(2\sqrt{2F/A})} \quad (32)$$

for the mean number of particles on the grain, and

$$\eta = \frac{2A}{F} \langle N(N-1) \rangle = \frac{I_{W/A+1}(2\sqrt{2F/A})}{I_{W/A-1}(2\sqrt{2F/A})} \quad (33)$$

for the recombination efficiency $\eta = 2R_{\text{master}}/F$ with R_{master} as in (4). $I_\nu(z)$ are modified Bessel functions. The crucial improvement we introduce is the consistent substitution of A via (6) instead of (1). A convenient and physically sensible parameter for the impingement flux consists in f/W , where f is the (effective) flux per site as defined by $F = fS$. Our full set of parameters now includes W/a , f/W and S .

For easiest comparison with previous work in the field, we employ the following standard scenario: We assume desorption and hopping to be thermally activated by the grain temperature T ,

$$W = \nu \exp\left(-\frac{E_1}{k_B T}\right), \quad a = \nu \exp\left(-\frac{E_0}{k_B T}\right), \quad (34)$$

with a uniform attempt frequency of $\nu = 10^{12} \text{ s}^{-1}$. In an analysis of temperature-programmed desorption experiments Katz et al. (1999) found the activation energies for an olivine surface to be $E_0/k_B = 287 \text{ K}$ and $E_1/k_B = 373 \text{ K}$. The situation in an interstellar gas cloud with H atoms in the gas phase at a temperature of 100 K is adopted from Biham et al. (2001) and leads to an effective flux of $f = 1.8 \times 10^{-9} \text{ s}^{-1}$. Altogether the physical parameters are thereby given as

$$\frac{W}{a} = \exp\left(-\frac{86 \text{ K}}{T}\right), \quad \frac{f}{W} = \exp\left(\frac{373 \text{ K}}{T} - 47.665\right). \quad (35)$$

5.1 Size dependence

We will first treat the size dependence of the recombination efficiency η for given temperature $T = 10 \text{ K}$ of the grain. One can see in Fig. 3 that, first, the true sweeping rate leads to a reduced recombination efficiency as compared to the conventional approximation in any case. Second, the quick decrease in the efficiency as one passes from large grains (in terms of a/W) to smaller sizes is shifted to the left, meaning that now, relative to the overall efficiency, smaller grains have gained in importance. For the sake of completeness we have further plotted the efficiency as predicted by the rate

equation treatment, i.e. $\eta_{\text{rateeq}} = 2R_{\text{rateeq}}/F$ with R_{rateeq} given by (3), and $\langle N \rangle$ obtained as the stationary solution of (2). Clearly, using the conventional approximation of the sweeping rate then eliminates all dependence of η_{rateeq} on the size of the grain. Choosing the true sweeping rate however results in the smaller grains even surpassing the larger ones in recombination efficiency, as the size dependence is then solely based on that of the reduction factor $A/(a/S)$, cf. Fig. 2. This illustrates once more that the replacement of the approximate by the true sweeping rate accounts for a different aspect of the problem (and is of most concern in a different regime) than the transition from the rate equation to the master equation treatment, as we already mentioned at the end of Sect. 4.

Finally, one can compare our plots with data obtained in simulations performed by Chang et al. (2005), using a continuous-time random walk algorithm. The efficiency we obtain for a square lattice is reasonably close to the results of their simulations, which backs their assertion that indeed it is back-diffusion that significantly undermines the recombination efficiency. However, our approach does not reproduce the striking difference between a square and a triangular lattice in the way that the simulations have shown (with the triangular lattice giving rise to much more effective recombination).

The origin of this discrepancy is not clear to us at present. However, we would like to rule out the possibility that it is an inherent shortcoming of the continuum approximation. While it is true that the transition from a lattice random walk to a continuous diffusion picture obliterates the fundamental differences of lattice types, many properties of a random walk are immune to this process. In particular, we have seen in Sect. 4.1 that the effect of the lattice type that is most important to us (the different number of distinct visited sites) is accurately represented by the lattice factor g in our model.

As we argued there, the large grain value for the true sweeping rate should be given by $A \approx WN_{\text{dis}}/S$, and the residence time is $t_{\text{res}} \approx 1/W$. It follows immediately that the asymptotic value of A for a triangular lattice should be larger than that for a square lattice by a factor of $2/\sqrt{3} \approx 1.15$, which is the ratio of the respective values of g or C^{-1} . Since for large enough grains the solution of the master equation yields $\eta \approx 2AF/W^2$ (Biham & Lipshtat 2002), this factor should reappear in the efficiencies, which is in good agreement with Fig. 3. Judging from the asymptotic values for large grains, the marginal difference in recombination efficiency between the square and the triangular lattice therefore is a reasonable outcome. Genuine lattice random walks cannot be expected to yield a significantly larger relative difference than our model predicts.

5.2 Temperature dependence

The temperature dependence of the recombination efficiency is another interesting aspect: Ultimately, from an astrophysical point of view the puzzle of hydrogen recombination in interstellar dust clouds is about the temperature window in which this process is efficient. Chang et al. (2005) found that their simulations gave very similar results compared to Biham et al. (2001) in the efficiency peak, while for higher temperatures the efficiency was somewhat smaller,

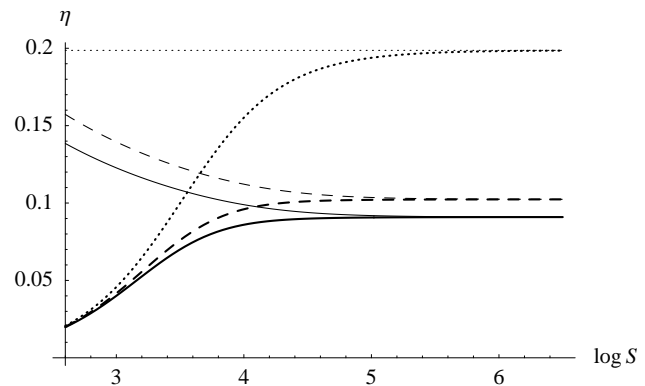


Figure 3. Recombination efficiency η as a function of the grain size S on a 10 K olivine grain in the standard scenario. The thick lines show $\eta(S)$ as computed with the master equation and the true sweeping rate, the continuous line standing for a square, the dashed one for a triangular lattice. The thick dotted graph was plotted using a/S as in Biham et al. (2001). The corresponding thin lines show the predictions of the rate equation treatment for the respective choice of sweeping rate.

and again differs for the different lattice types (both effects as expected in our model as well, judging from the fixed-temperature plot in Fig. 3). We focus here on the comparison of the analytical results for the different sweeping rate expressions.

It should be noted first of all that we do *not* include the mechanism of Langmuir-Hinshelwood (LH) rejection. This mechanism repels H atoms that impinge on occupied adsorption sites on the grain surface and is responsible for a quick decay of the recombination efficiency for very low temperatures, where desorption is heavily suppressed and the H (and H₂) coverage on the grain is large.

As we neglect this effect and treat a fixed grain size (and therefore a fixed impingement flux), the remaining factors governing the recombination efficiency are the relation between the fixed S and the temperature-dependent W/a , and the average number of reactants on the grain, which is smaller than, but of the order of F/W . As the temperature increases, W/a increases as well and we approach the regime of large grains (cf. Sect. 4.1) with the resulting small encounter probability. Combined with the decreasing F/W this prohibits efficient recombination. For lower temperatures we head towards the regime of small grains, where an encounter probability near unity and an increasing number of reactants predict a large recombination efficiency. No finite temperature completely prohibits diffusion; and due to the larger activation energy, desorption is suppressed even more. Diffusion will almost always let two atoms meet once they are on the surface, and the extremely long time this might take at very low temperatures is a hidden feature when treating steady-state conditions.

LH rejection should be negligible for temperatures roughly at or larger than the peak efficiency temperature (Biham et al. 2001), so we can expect our results to validly show the breakdown for higher temperatures. A rough estimate for a temperature below which our results fail can be obtained using (35). The mean coverage of H atoms on the grain is of the order of f/W . The temperature at which this coverage becomes of the order of unity surely is beyond the

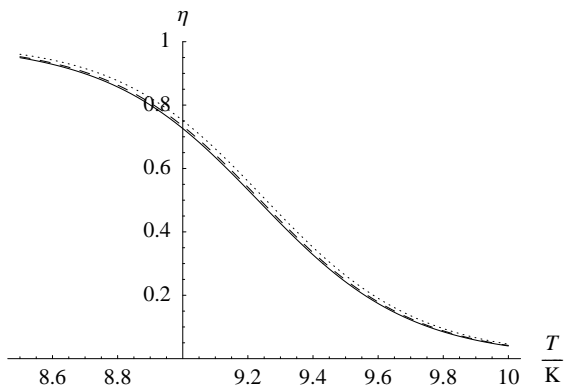


Figure 4. Recombination efficiency as a function of the temperature T , for a grain of $S = 10^3$ sites. Again, the continuous line shows the master equation result with the true sweeping rate and a square lattice, the dashed line represents the result for a triangular lattice, and the dotted line uses the conventional approximation. Note that this plot is horizontally stretched to uncover the small differences. The regime of large grains only starts at higher temperatures outside the plotted region.

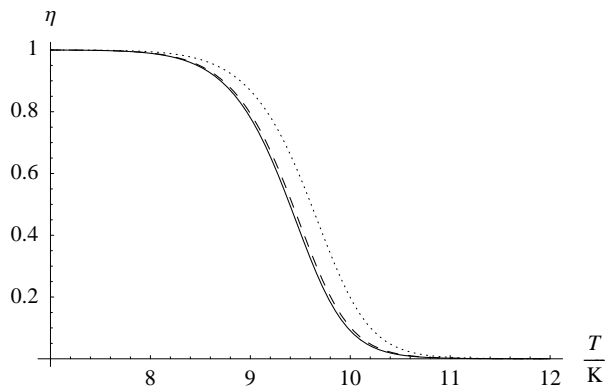


Figure 5. The same plot as in Fig. 4, now for a grain of size $S = 10^6$ sites. This size is ‘large’ for practically all shown temperatures.

validity of our assumptions, and this temperature is given by $T_{\text{LH}} \approx 7.8$ K.

For a rather small grain of 1000 adsorption sites (Fig. 4), differences in the various predictions of the recombination efficiency are very small, and we increased the resolution by restriction to a very narrow temperature range. The above estimate suggests that the breakdown of η for $T > 8$ K should also apply to an analogous model incorporating LH rejection. On a larger grain with 10^6 adsorption sites (Fig. 5) one can see that recombination ceases to be effective at a lower temperature when employing the true sweeping rate rather than the conventional approximation (differences between the lattice types are still hardly perceptible). That this effect only occurs for larger grains is explicable with the help of Fig. 3, which showed that outside the efficiency peak, the reduction (of A with respect to a/S) is most pronounced for large grains, since only then back-diffusion becomes effective. On the other hand our earlier explanations imply that (independent of the fixed grain size) as we increase or decrease the temperature, the efficiency has to approach

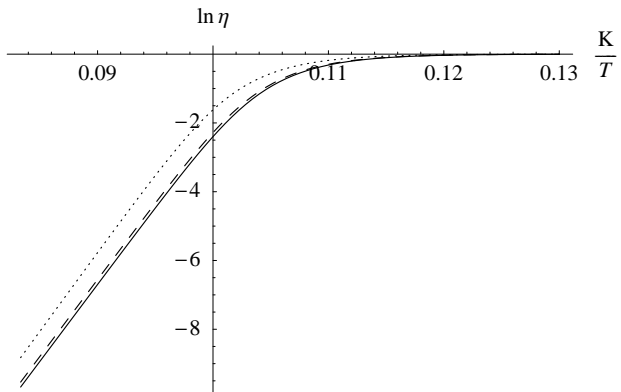


Figure 6. An Arrhenius plot of the recombination efficiency under the previous conditions.

the limits zero and unity, respectively. Using the conventional approximation $A = a/S$ in (5) yields the quantity $1/(1 + SW/a)$ as a substitute for the encounter probability, which shares the limiting behaviour of p_{enc} used in the argument. Hence in both limits, the efficiency is the same for the two sweeping rate concepts. A fairly general suggestion of the figures is that grain size hardly seems to matter for the upper bound of the temperature range of effective recombination: A difference of three orders of magnitude of the number of adsorption sites results in only a minute change of the upper temperature bound.

Finally, we re-plot the last graph in the Arrhenius fashion, i.e. as $\ln \eta(1/T)$, which is shown in Fig. 6. For rising temperature (in the left part of the plot) there exists an effective (negative) activation energy, which can be read off to be $E_{\text{act}}/k_{\text{B}} \approx -440$ K. Using the large-grain value $\eta \approx 2AF/W^2$ together with (27) and (34) yields the prediction $(E_0 - 2E_1)/k_{\text{B}} = -459$ K for this energy, in good accordance with the estimate.

For this astrophysical setting, we may sum up the effect of employing the true sweeping rate (6) instead of (1) as follows: At a given temperature, relative to the decreased overall efficiency, smaller grains gain in importance for the recombination process, since larger grains are more affected by back-diffusion. With a fixed grain size, the correction is only pronounced for (absolutely) large grains, but does not change the upper temperature bound of efficient recombination considerably. This bound rather seems very sensitive to a more detailed modelling of the complex surface structure (Chang et al. 2005; Perets & Biham 2006). Our results thus strengthen the claim that hydrogen formation on dust grains crucially depends on the grain surface structure.

6 CONCLUSIONS

We could show that it is possible to rigorously define the true sweeping rate for diffusion-mediated reactions on a dust grain surface, and for a spherical homogeneous grain, it could be evaluated exactly. The primary effect of the spatial structure of the problem consists in a reduction of the true sweeping rate compared to the conventional approximation, which is due to the back-diffusion of randomly walking atoms. This reduction is moderate and dependent on the size

of the grain for small grains, whereas for increasing grain size it grows stronger before saturating at a value dependent on the ratio of the rates of hopping and desorption of reactants.

The picture of a spherical, homogeneous grain is highly idealized, as is the assumption of a single reaction type, but since the effects we have found have explanations that remain reasonable for any type of grain and with a very general reaction network, we expect the results to remain relevant as well.

Applying the model specifically to the recombination of hydrogen atoms on interstellar dust grains, we could compare the recombination efficiency that our model predicts with the results of microscopic Monte Carlo simulations. We found that they coincide reasonably well for a square lattice of adsorption sites, but that we cannot reproduce, and have no explanation for, the substantially increased efficiency on an (otherwise equal) triangular lattice simulations have shown.

In the wake of the decreased true sweeping rate (compared to the conventional approximation), the efficiency is reduced as well. Least affected by this reduction, small grains become more important for the recombination process. For a given size of the grain however, the upper temperature bound of efficient formation of molecular hydrogen is hardly changed.

For an improved quantitative analysis, the complex surface structure of interstellar dust grains seems to be of paramount importance. It might be a worthwhile enterprise to consider more complicated analytical models which can incorporate some of these aspects. A possible next step would be the replacement of a single binding energy and diffusion barrier by energy distributions, accounting for the inhomogeneity of the lattice of adsorption sites on the grain, as has been done in simulations (Chang et al. 2005). Another interesting approach focuses on the effect of the porosity of the dust grains (Perets & Biham 2006).

ACKNOWLEDGMENTS

We thank E. Herbst for useful discussions and Q. Chang for correspondence.

APPENDIX A: LATTICE GEOMETRY

Assuming S to be large, so that curvature effects do not play any role for the single atomic ‘tile’, we can cover a surface area $4\pi R^2$ by simply dividing it into such tiles, each of the area that a single atom occupies. This tile area depends on the distance of (the centers of) nearest neighbor sites, $2r$, and the lattice type. Elementary trigonometry shows that, for a hexagonal lattice (which by common terminology refers to a ‘honeycomb’ lattice formed by the adsorption sites, with coordination number 3), it is given by $3\sqrt{3}r^2$, for a square lattice it is obviously $4r^2$, and a triangular lattice (i.e. one with coordination number 6) has a tile area of $2\sqrt{3}r^2$. So we have $S = g(2R/r)^2$ with a factor $g = \pi/(3\sqrt{3})$ for the hexagonal, $\pi/4$ for the square, and $\pi/(2\sqrt{3})$ for the triangular lattice, which is smaller than but of the order of unity in all three cases.

APPENDIX B: ASYMPTOTIC EXPANSION

Asymptotic expansions of the Legendre functions near their singularity are given as equations 3.9.1 (13)ff. in Erdélyi (1953). Since it was not clear from the outset that the degree of these expansions sufficed, we extended the expansion with the aid of computer algebra, and en route found a misprint (not accounted for in the errata) in equation (15) *ibid.*, which erroneously lacks a factor of 2 preceding Euler’s constant, cf. (B2)f. below.

We rewrite (16) as

$$p_{\text{enc}} = \left\{ \frac{1-z^2}{2\nu(\nu+1)} \frac{d}{dz} [\ln P_\nu(z)] + \frac{1+z}{2} \right\}_{z=-\cos(r/R)}, \quad (\text{B1})$$

and then use *Mathematica* to expand the encounter probability to first order in $(1+z)$ about 0, keeping ν fixed. To cast the result into a reasonable form, we manually apply various transformations (valid for arbitrary complex ν) to get rid of all Γ and most ψ functions, viz. $\Gamma(1 \mp \nu) = \pm\pi / [\sin(\nu\pi)\Gamma(\pm\nu)]$, $\psi(\pm\nu) = \psi(1 \pm \nu) \mp 1/\nu$, and $\psi(1 \mp \nu) = \psi(\pm\nu) \pm \pi \cot(\nu\pi)$.

Now we identify $u = (1+z)/2$, and with the definition

$$X = \ln u^{-1} - 2\gamma - 2\psi(\nu+1) - \pi \cot(\nu\pi) \quad (\text{B2})$$

[the square brackets in (17)] we obtain

$$p_{\text{enc}} \approx \frac{1}{-\nu(\nu+1)X} + \frac{1+2\nu(\nu+1)+2\nu(\nu+1)X}{-\nu(\nu+1)X^2} \cdot u \quad (\text{B3})$$

as the expansion of the encounter probability up to linear order in $u \approx [r/(2R)]^2$. The zeroth order term is equivalent to equation (17) and describes a non-trivial behaviour that we examine in the main text. The remaining question is why the next order is not needed in either of the two regimes discussed in Sect. 3.3. As in the main text, we regard the $\ln u^{-1}$ term as being of the order of unity (cf. footnote 5).

For large grains, there is no need to include terms of $\mathcal{O}(u)$: X then is of $\mathcal{O}(1)$ as shown in the main text, while $-\nu(\nu+1) = (R/\ell_D)^2 \gg 1$. The largest contribution of the second term thence has an additional factor of $-\nu(\nu+1)u \approx [r/(2\ell_D)]^2 \ll 1$ compared to the first summand.

The small grain regime requires a bit more effort, since ν and u can generally be of comparable order now. Expanding about $\nu \rightarrow 0-$, we have $\psi(1+\nu) = -\gamma + \mathcal{O}(\nu)$ so that $X = \ln u^{-1} - 1/\nu + \mathcal{O}(\nu)$. Hence $-\nu X = 1 - \nu \ln u^{-1} + \mathcal{O}(\nu^2)$ and $(\nu+1)X = -1/\nu + \ln u^{-1} - 1 + \mathcal{O}(\nu) = -1/\nu[1 - \nu(\ln u^{-1} - 1) + \mathcal{O}(\nu^2)]$. The $\mathcal{O}(u^0)$ term thus reads $1 + \nu(\ln u^{-1} - 1) + \mathcal{O}(\nu^2)$. Similarly evaluating the $\mathcal{O}(u^1)$ terms yields the pre-factor $\nu[1 - \nu + \mathcal{O}(\nu^2)]$: Without a contribution of $\mathcal{O}(\nu^0 u^1)$ present, this is but a higher order correction to the first summand. One can further see that the direct impingement term u included in (16) is of precisely that order, and thence must have gone to cancel a corresponding term of the expression (15). Altogether we have shown that (17) of the main text contains all necessary terms to consistently perform the subsequent approximations.

REFERENCES

- Biham O., Furman I., Katz, N., Pirronello V., Vidali G., 1998, MNRAS, 296, 869
 Biham O., Furman I., Pirronello V., Vidali G., 2001, ApJ, 553, 595

- Biham O., Lipshtat A., 2002, Phys. Rev. E, 66, 056103
Biham O., Krug J., Lipshtat A., Michely T., 2005, Small, 1, 502
Caselli P., Hasegawa T.I., Herbst E., 1998, ApJ, 495, 309
Chang Q., Cuppen H.M., Herbst E., 2005, A&A, 434, 599
Charnley S.B., Tielens A.G.G.M., Rodgers S.D., 1997, ApJ, 482, L203
Cuppen H.M., Herbst E., 2005, MNRAS, 361, 565
Erdélyi A., ed., 1953, Higher Transcendental Functions, vol. 1. McGraw-Hill, New York
Gradshteyn I.S., Ryzhik I.M., 2000, Table of Integrals, Series, and Products, 6th edn. Academic Press, San Diego
Green N.J.B., Toniazzi T., Pilling M.J., Ruffle D.P., Bell N., Hartquist T.W., 2001, A&A, 375, 1111
Herbst E., Shematovich V.I., 2003, Ap&SS, 285, 725
Hughes B.D., 1995, Random Walks and Random Environments, vol. 1. Oxford University Press, Oxford
Katz N., Furman I., Biham O., Pirronello V., Vidali G., 1999, ApJ, 522, 305
Krug J., Politi P., Michely T., 2000, Phys. Rev. B, 61, 14037
Krug J., 2003, Phys. Rev. E, 67, 065102(R)
Lipshtat A., Biham O., 2004, Phys. Rev. Lett., 93, 170601
Michely T., Krug J., 2004, Islands, Mounds and Atoms. Patterns and Processes in Crystal Growth Far from Equilibrium. Springer, Berlin
Montroll E.W., Weiss G.H., 1965, J. Math. Phys., 6, 167
Perets H.B., Biham O., 2006, MNRAS, 365, 801
Pickles J.B., Williams D.A., 1977, Ap&SS, 52, 443
Stantcheva T., Caselli P., Herbst E., 2001, A & A, 375, 673
Tielens A.G.G.M., Hagen W., 1982, A&A, 114, 245
Vidali G., Roser J., Manicó G., Pirronello V., Perets H.B., Biham O., 2005, J. Phys.: Conf. Ser., 6, 36